

Infrared signature of the superconducting gap symmetry in iron-arsenide superconductors

Y. M. Dai,^{1,2} B. Xu,¹ B. Shen,¹ H. H. Wen,^{1,3} X. G. Qiu,¹ and R. P. S. M. Lobo^{2,*}

¹*Beijing National Laboratory for Condensed Matter Physics,
National Laboratory for Superconductivity, Institute of Physics,
Chinese Academy of Sciences, P.O. Box 603, Beijing 100190, China*

²*LPEM, ESPCI-ParisTech, CNRS, UPMC, 10 rue Vauquelin, F-75231 Paris Cedex 5, France*

³*National Laboratory of Solid State Microstructures and Department of Physics, Nanjing University, Nanjing 210093, China*

(Dated: June 23, 2011)

We measured the *in-plane* optical conductivity of a nearly optimally doped $\text{Ba}_{0.6}\text{K}_{0.4}\text{Fe}_2\text{As}_2$ single crystal with $T_c = 39.1$ K. Upon entering the superconducting state the optical conductivity below ~ 20 meV vanishes, strongly suggesting a fully gapped system. A BCS-like fit requires two different isotropic gaps to describe the optical response of this material. The temperature dependence of the gaps and the penetration depth suggest a strong interband coupling, but no impurity scattering induced pair breaking is present. This contrasts to the large residual conductivity observed in optimally doped $\text{Ba}(\text{Fe}_{1-x}\text{Co}_x)_2\text{As}_2$ and strongly supports an s_{\pm} gap symmetry for these compounds.

PACS numbers: 74.20.Rp, 74.70.Xa, 74.25.Gz

A crucial issue in the superconducting mechanism of iron-arsenide compounds is understanding the properties of the superconducting gap(s). Electronic structure calculations predict that multiple bands at the Fermi Level participate in the formation of the condensate [1, 2], leading to multigap superconductivity. Mazin et al. [3] suggested an antiferromagnetic spin fluctuation mediated superconductivity in these materials resulting in a possible sign reversal between the order parameters in different Fermi surface sheets, in the so-called s_{\pm} symmetry. This s_{\pm} symmetry has an important pair-breaking consequence. When scattering by non-magnetic impurity between bands having s_{+} and s_{-} symmetries takes place, Cooper pairs are annihilated and an excess of unpaired quasiparticles appear in the superconducting state [4].

In this sense, BaFe_2As_2 based materials are of utmost importance as superconductivity appears with in- and out-of- FeAs plane doping. Angle resolved photoemission spectroscopy (ARPES) finds multiple nodeless gaps in both $\text{Ba}(\text{Fe}_{1-x}\text{Co}_x)_2\text{As}_2$ [5] and $\text{Ba}_{1-x}\text{K}_x\text{Fe}_2\text{As}_2$ [6, 7] in accordance with theoretical calculations [8] that predict isotropic gaps in optimally doped Co and K materials. Yet, their spectroscopic responses are strikingly different.

In $\text{Ba}(\text{Fe}_{1-x}\text{Co}_x)_2\text{As}_2$, Co atoms go into the FeAs planes. This material shows a V-shaped density of states [9] that produces a strong sub-gap absorption [10, 11]. An extensive set of optical conductivity data exists on this family [11–18] showing multiple superconducting gaps and, most importantly, sub-gap extra absorption in the superconducting state.

$\text{Ba}_{1-x}\text{K}_x\text{Fe}_2\text{As}_2$ represents a different situation as doping K atoms sit out of the FeAs planes. In addition to ARPES, local magnetization [19]; point-contact Andreev reflection [20]; specific heat [21, 22]; scanning tunneling microscopy [23]; and thermal transport [24] point

towards multiple fully open gaps. These measurements show that two superconducting gaps with different values dominate the physics of $\text{Ba}_{1-x}\text{K}_x\text{Fe}_2\text{As}_2$: a smaller gap in the $2\Delta/k_B T_c$ of 1.3–4.2 and a larger gap in the $2\Delta/k_B T_c$ in the 4.5–10 ranges.

Should we expect any fundamental difference between $\text{Ba}(\text{Fe}_{1-x}\text{Co}_x)_2\text{As}_2$ and $\text{Ba}_{1-x}\text{K}_x\text{Fe}_2\text{As}_2$ families? In particular, can the different location of dopant atoms shed any light on the claimed s_{\pm} symmetry?

Optical conductivity is a very sensitive probe to charge carriers at low energies and should provide a direct information on unpaired carriers in the superconducting state. Opposite to $\text{Ba}(\text{Fe}_{1-x}\text{Co}_x)_2\text{As}_2$, very few optical measurements exist on $\text{Ba}_{1-x}\text{K}_x\text{Fe}_2\text{As}_2$. Yang et al. [25] measured the infrared response of this system above T_c only and found that the charge carriers are coupled to a broad bosonic spectrum extending beyond 100 meV with a very large coupling constant at low temperature. Li et al. [26] found a fully open gap but could not quantify the presence of multiple superconducting gaps. Charnukha et al. [27] described their ellipsometry data with two gaps, however, one of them is below their lowest measured frequency.

In this letter, we present a detailed infrared study on a nearly optimally doped $\text{Ba}_{0.6}\text{K}_{0.4}\text{Fe}_2\text{As}_2$ single crystal. Below T_c , we observe a fully open gap below 20 meV, but in order to describe the optical conductivity a second gap at 33 meV has to be considered. The temperature dependence of the gap values indicates a strong interband interaction in $\text{Ba}_{1-x}\text{K}_x\text{Fe}_2\text{As}_2$. The fully open gap response indicates the absence of impurity induced pair breaking. We show that K and Co doped BaFe_2As_2 have strikingly different far-infrared properties. In the former impurities are out of the FeAs plane and, therefore, no interband pair-breaking scattering exists. In the

latter, existence of in-plane impurity scattering leads to pair breaking. Our results provide a strong indication that the gap symmetry in iron-arsenide superconductors is s_{\pm} .

High quality single crystals of $\text{Ba}_{0.6}\text{K}_{0.4}\text{Fe}_2\text{As}_2$ were grown by an FeAs flux method [28]. The resistivity of the crystal (solid line in the lower inset of Fig. 1) shows a very sharp superconducting transition with an onset at $T_c = 39.1$ K and a width $\Delta T_c \sim 0.5$ K. Near normal incidence reflectivity from 20 cm^{-1} to 12000 cm^{-1} was measured on Bruker IFS113 and IFS66v spectrometers at 19 different temperatures from 5 to 300 K. The absolute reflectivity of the sample was obtained with an *in situ* gold overfilling technique [29]. The reflectivity has an absolute accuracy better than 0.5% and a relative accuracy better than 0.1%. The data was extended to the visible and UV range (10000 cm^{-1} to 55000 cm^{-1}) at room temperature with an AvaSpec-2048 \times 14 model fiber optic spectrometer. The sample was cleaved prior to each temperature run. We complemented the above data by measuring the reflectivity, normalized by its value at 40 K, every Kelvin from 5 to 45 K in the $70\text{--}700 \text{ cm}^{-1}$ range. We then used the absolute reflectivity at 40 K to correct the data taken at all other temperatures. These measurements have a very high relative accuracy and allow for a fine determination of the spectral temperature evolution.

Figure 1 displays the reflectivity of $\text{Ba}_{0.6}\text{K}_{0.4}\text{Fe}_2\text{As}_2$ on the *ab*-plane above and below T_c . Upon entering the superconducting state, the reflectivity increases and reaches a flat unity response below $\sim 20 \text{ meV}$, which is a clear signature of a fully open superconducting gap [30, 31].

The real part $[\sigma_1(\omega)]$ of the optical conductivity was derived from the reflectivity through Kramers-Kronig analysis. At low frequencies we used either a Hagen-Rubens ($1 - A\sqrt{\omega}$) or a superconducting ($1 - A\omega^4$) extrapolation. At high frequencies we used a constant reflectivity to 40 eV followed by a ω^{-4} free electron termination. Figure 2 shows $\sigma_1(\omega)$ at various temperatures. Error bars at selected frequencies are shown at 35 K (temperature where they are the largest). These error bars were estimated assuming different high and low frequency extrapolations and an error of 0.5% in the value of the absolute reflectivity.

Above T_c , $\sigma_1(\omega)$ shows a Drude-like metallic response described by a Drude-Lorentz model:

$$\sigma_1(\omega) = \frac{2\pi}{Z_0} \sum_k \left[\frac{\Omega_{p,k}^2}{\tau_k(\omega^2 + \tau_k^{-2})} + \frac{\gamma_k \omega^2 S_k^2}{(\Omega_k^2 - \omega^2)^2 + \gamma_k^2 \omega^2} \right], \quad (1)$$

where Z_0 is the vacuum impedance. The first term in Eq. 1 corresponds to a sum of free-carrier Drude responses, each characterized by a plasma frequency ($\Omega_{p,k}$) and a scattering rate (τ_k^{-1}). The second term is a sum of Lorentz oscillators characterized by a resonance frequency (Ω_k), a line width (γ_k) and a plasma frequency

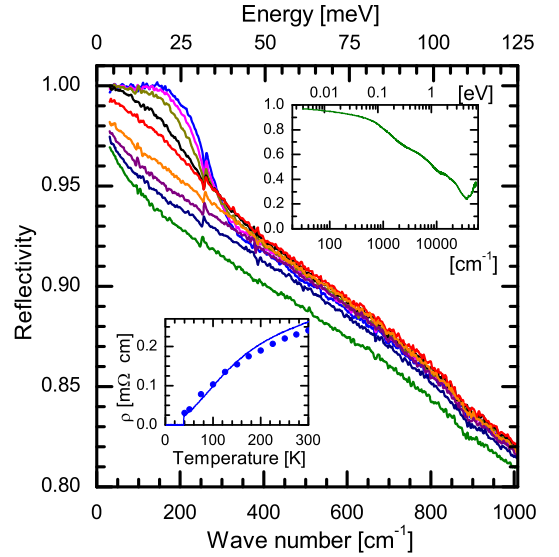


Figure 1. (color online) $\text{Ba}_{0.6}\text{K}_{0.4}\text{Fe}_2\text{As}_2$ infrared reflectivity measured (from top to bottom) at 4, 25, 30, 35, 40, 100, 150, 200, and 300 K. The top inset shows the reflectivity at 300 K up to 7.5 eV. The solid line in the lower inset is the dc resistivity and the solid circles are values from the zero frequency extrapolation of the optical conductivity.

(S_k). Although band structure theory predicts up to 5 bands at the Fermi Level [1, 2], two Drude terms are enough to describe the optical conductivity of iron-arsenide superconductors [12]. We also used one Lorentz oscillator to represent the phonon at about 30 meV and another oscillator to account for mid-infrared interband transitions. These four contributions can account for the optical conductivity up to 1.25 eV at all measured temperatures in the normal state. Fits obtained for the normal state with Eq. 1 are shown as the solid smooth lines in Fig. 2. The zero frequency values of our fits represent the inverse dc resistivity of the material which we compare (solid circles in the lower inset of Fig. 1) to the measured dc resistivity (solid line). The very good agreement indicates that our parametrization of the data is representative of the physics of the system.

Below T_c , a dramatic suppression of $\sigma_1(\omega)$ sets in. At 5 K $\sigma_1(\omega)$ vanishes, within error bars, below 20 meV indicating a fully open gap. In order to quantitatively describe the optical response below T_c , we replaced the two Drude terms used for the normal state in Eq. 1 by two corresponding Mattis-Bardeen conductivities, modified to take into account arbitrary scattering [32]. The fits obtained for $\sigma_1(\omega)$ in the superconducting state are also shown as solid smooth lines in Fig. 2. The inset details the four contributions (two superconducting bands, one phonon and the mid-infrared interband transition) needed to describe $\sigma_1(\omega)$ at 5 K. The superconducting response is composed of two isotropic gaps at $\Delta_0^S = 10 \text{ meV}$ and $\Delta_0^L = 16.5 \text{ meV}$. We note that the gap values deter-

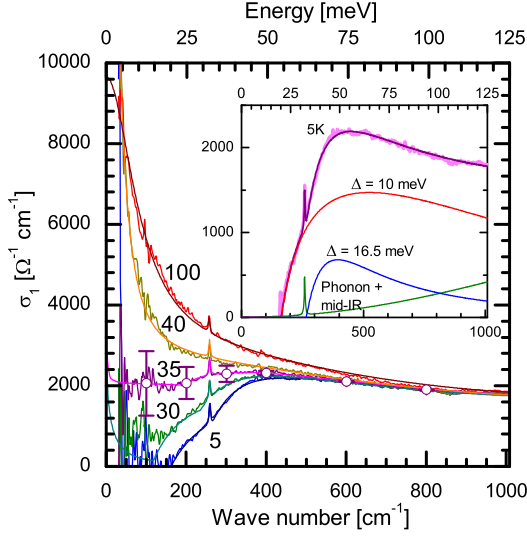


Figure 2. (color online) $\text{Ba}_{0.6}\text{K}_{0.4}\text{Fe}_2\text{As}_2$ optical conductivity above and below T_c . The smooth lines through the data are fits assuming that mobile charges are described by either Drude (normal state) or Mattis-Bardeen (superconducting) carriers. The inset decomposes the total fit of the optical conductivity at 5 K into individual contributions. Note the a change of slope in $\sigma_1(\omega)$ at twice the value of the highest gap, $2\Delta_0^L = 33$ meV.

mined here yield $2\Delta_0^S/k_B T_c = 5.9$ and $2\Delta_0^L/k_B T_c = 9.8$, values larger than the BCS weak coupling limit but well within the reported range for this material [6, 7, 19–23].

Let us now analyze our results in the framework of the BCS theory. The top panel of Fig. 3 shows the temperature dependence of the gaps obtained from the fits to $\sigma_1(\omega)$. The solid lines are an approximate strong coupling correction to the BCS behavior, obtained by plugging the experimental values for $\Delta(0)$ and T_c into the BCS gap equation. Although the fit is not perfect it reproduces well the rapid gap opening below T_c expected for a strongly coupled superconductor [33]. Moreover, a significant interband interaction matrix element is indicated by the temperature dependence of the small gap. In a two gap system where the bands are weakly interacting the small gap decreases rapidly well below T_c [34]. The effect of a strong interband coupling is to make the small gap temperature dependence follow the large gap, as seen here.

The lower panel in Fig. 3 depicts the penetration depth for $\text{Ba}_{0.6}\text{K}_{0.4}\text{Fe}_2\text{As}_2$. The dashed line is the solution of the penetration depth BCS equation with $\Delta_0 = 10$ meV whereas the solid line assumes $\Delta_0 = 16.5$ meV. In the inset we show the superfluid density and the same calculations as in the main panel. The calculation with the large gap Δ_0^L gives a better description to the data. This is a signature that the superconducting bands respond in parallel as implied when we described $\sigma_1(\omega)$ by the sum of two Mattis-Bardeen terms. The larger gap, hav-

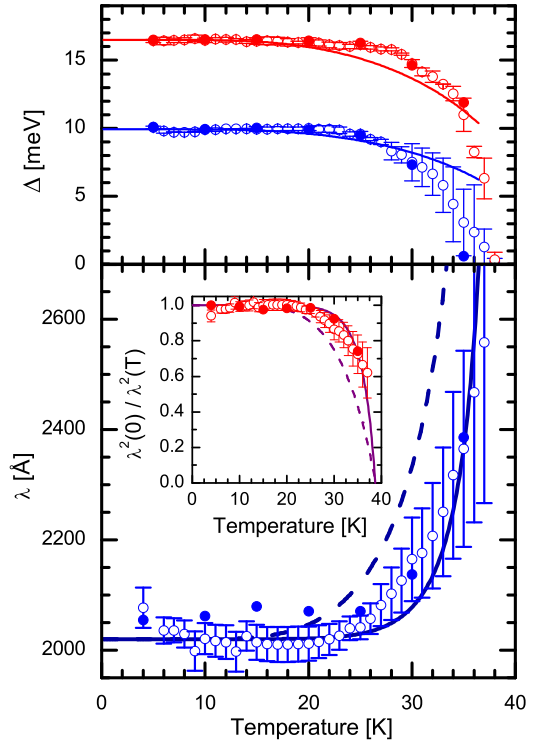


Figure 3. (color online) The top panel shows the superconducting gap values obtained by fitting σ_1 obtained from the fine reflectivity temperature resolution measurements (open symbols) and from the accurate absolute reflectivity (solid symbols). The solid lines are an approximate strong coupling correction to the BCS gap equation. The bottom panel shows the penetration depth calculated from the London plasma frequency. Solid and open symbols have the same meaning as in the top panel. The dashed line is a calculation with $\Delta_0^S = 10$ meV and the solid line with $\Delta_0^L = 16.5$ meV. The inset shows the superfluid density and the same calculations as in the main panel.

ing a smaller penetration depth, dominates the value of the total penetration depth.

It is very instructive to compare the fully open gap observed in $\text{Ba}_{0.6}\text{K}_{0.4}\text{Fe}_2\text{As}_2$ where dopants are out of the FeAs planes, to $\text{Ba}(\text{Fe}_{1-x}\text{Co}_x)_2\text{As}_2$ where dopants are in the FeAs planes. Figure 4 shows the optical conductivity for both materials at 5 K. In $\text{Ba}_{0.6}\text{K}_{0.4}\text{Fe}_2\text{As}_2$ σ_1 vanishes, within error bars, below the smaller gap absorption threshold ($2\Delta_0^S$). Hence, there is no sign of unpaired carriers in the superconducting state. Conversely, the data for $\text{Ba}(\text{Fe}_{1-x}\text{Co}_x)_2\text{As}_2$ (Ref. 11) shows a large low energy, sub-gap, absorption in the superconducting state. This extra absorption is described by a Drude peak characterizing the unpaired carriers. Therefore, the in-plane impurity scattering is strong in $\text{Ba}(\text{Fe}_{1-x}\text{Co}_x)_2\text{As}_2$ and it induces pair-breaking that is, at least partially, responsible for the residual low frequency specific heat [35] observed in that system. In $\text{Ba}_{1-x}\text{K}_x\text{Fe}_2\text{As}_2$ K atoms stay out of

the FeAs planes and hence no interband impurity scattering is expected. In this case no pair-breaking induced residual low frequency $\sigma_1(\omega)$ is present. In both materials dopants are non magnetic and hence should not be pair-breaking scattering centers. The fact that when the dopant is in the FeAs plane creates unpaired quasiparticles matches naturally the s_{\pm} gap symmetry proposed for iron-arsenide superconductors.

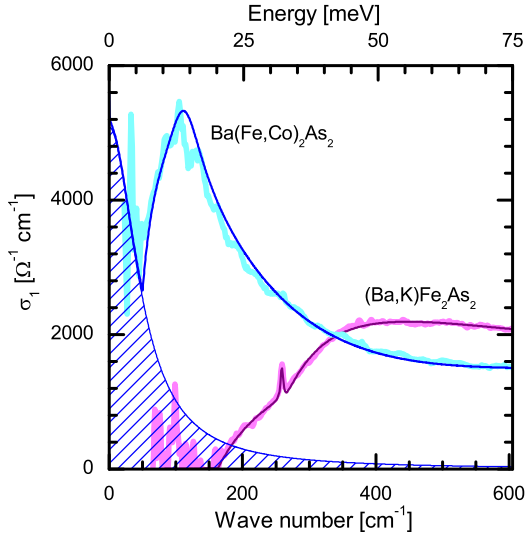


Figure 4. (color online) Optical conductivity at 5 K for $\text{Ba}(\text{Fe}_{0.92}\text{Co}_{0.08})_2\text{As}_2$ (Ref. 11) and $\text{Ba}_{0.6}\text{K}_{0.4}\text{Fe}_2\text{As}_2$. For the latter, the thin solid lines are a fit as described in the text. For the former, besides the superconducting Mattis-Bardeen response, a Drude term (shown as the dashed area) is necessary to describe the residual sub-gap absorption in the superconducting state.

In summary, we presented a detailed optical study on a nearly optimally doped $\text{Ba}_{0.6}\text{K}_{0.4}\text{Fe}_2\text{As}_2$ single crystal. In the normal state, the optical response is metallic and can be well described by two Drude terms. In the superconducting state, an opening of two superconducting gaps was clearly observed. The optical conductivity vanishes roughly below 20 meV indicating fully open gaps. A strong coupling BCS analysis shows that two almost isotropic gaps with different values describe the optical response of our sample. The temperature dependence of the gaps indicates a strong interband interaction. We found that $\text{Ba}_{1-x}\text{K}_x\text{Fe}_2\text{As}_2$ out-of-plane K atoms do not induce pair-breaking whereas scattering by the in-plane Co atoms of $\text{Ba}(\text{Fe}_{1-x}\text{Co}_x)_2\text{As}_2$ deplete superconductivity. This result strongly supports an s_{\pm} symmetry for the gap.

We would like to acknowledge discussions with J. P. Carbotte and T. Timusk, and the financial support from the Science and Technology Service of the French Embassy in China. Work in Beijing was supported by the MOST and the National Science Foundation of China. Work in Paris was supported by the ANR under Grant

No. BLAN07-1-183876 GAPSUPRA.

* lobo@espci.fr

- [1] K. Haule, J. H. Shim, and G. Kotliar, Phys. Rev. Lett. **100**, 226402 (2008).
- [2] D. J. Singh and M.-H. Du, Phys. Rev. Lett. **100**, 237003 (2008).
- [3] I. I. Mazin, D. J. Singh, M. D. Johannes, and M. H. Du, Phys. Rev. Lett. **101**, 057003 (2008).
- [4] A. V. Chubukov, M. G. Vavilov, and A. B. Vorontsov, Phys. Rev. B **80**, 140515 (2009).
- [5] K. Terashima, Y. Sekiba, J. H. Bowen, K. Nakayama, T. Kawahara, T. Sato, P. Richard, Y.-M. Xu, L. J. Li, G. H. Cao, et al., Proceedings of the National Academy of Sciences **106**, 7330 (2009).
- [6] H. Ding, P. Richard, K. Nakayama, K. Sugawara, T. Arakane, Y. Sekiba, A. Takayama, S. Souma, T. Sato, T. Takahashi, et al., Europhys. Lett. **83**, 47001 (2008).
- [7] K. Nakayama, T. Sato, P. Richard, Y.-M. Xu, Y. Sekiba, S. Souma, G. F. Chen, J. L. Luo, N. L. Wang, H. Ding, et al., Europhys. Lett. **85**, 67002 (2009).
- [8] S. Maiti and A. V. Chubukov, Phys. Rev. B **83**, 220508 (2011).
- [9] Y. Bang, H.-Y. Choi, and H. Won, Phys. Rev. B **79**, 054529 (2009).
- [10] M. L. Teague, G. K. Drayna, G. P. Lockhart, P. Cheng, B. Shen, H.-H. Wen, and N.-C. Yeh, Phys. Rev. Lett. **106**, 087004 (2011).
- [11] R. P. S. M. Lobo, Y. M. Dai, U. Nagel, T. Rõm, J. P. Carbotte, T. Timusk, A. Forget, and D. Colson, Phys. Rev. B **82**, 100506 (2010).
- [12] D. Wu, N. Barišić, P. Kallina, A. Faridian, B. Gorshunov, N. Drichko, L. J. Li, X. Lin, G. H. Cao, Z. A. Xu, et al., Phys. Rev. B **81**, 100512 (2010).
- [13] E. van Heumen, Y. Huang, S. de Jong, A. B. Kuzmenko, M. S. Golden, and D. van der Marel, EPL (Europhysics Letters) **90**, 37005 (2010).
- [14] K. W. Kim, M. Rössle, A. Dubroka, V. K. Malik, T. Wolf, and C. Bernhard, Phys. Rev. B **81**, 214508 (2010).
- [15] D. Wu, N. Barišić, M. Dressel, G. H. Cao, Z. A. Xu, J. P. Carbotte, and E. Schachinger, Phys. Rev. B **82**, 184527 (2010).
- [16] J. J. Tu, J. Li, W. Liu, A. Punnoose, Y. Gong, Y. H. Ren, L. J. Li, G. H. Cao, Z. A. Xu, and C. C. Homes, Phys. Rev. B **82**, 174509 (2010).
- [17] T. Fischer, A. V. Pronin, J. Wosnitzer, K. Iida, F. Kurth, S. Haindl, L. Schultz, B. Holzapfel, and E. Schachinger, Phys. Rev. B **82**, 224507 (2010).
- [18] R. Valdés Aguilar, L. S. Bilbro, S. Lee, C. W. Bark, J. Jiang, J. D. Weiss, E. E. Hellstrom, D. C. Larbalestier, C. B. Eom, and N. P. Armitage, Phys. Rev. B **82**, 180514 (2010).
- [19] C. Ren, Z.-S. Wang, H.-Q. Luo, H. Yang, L. Shan, and H.-H. Wen, Phys. Rev. Lett. **101**, 257006 (2008).
- [20] P. Szabó, Z. Pribulová, G. Pristá, S. L. Bud'ko, P. C. Canfield, and P. Samuely, Phys. Rev. B **79**, 012503 (2009).
- [21] G. Mu, H. Luo, Z. Wang, L. Shan, C. Ren, and H.-H. Wen, Phys. Rev. B **79**, 174501 (2009).
- [22] P. Popovich, A. V. Boris, O. V. Dolgov, A. A. Golubov,

- D. L. Sun, C. T. Lin, R. K. Kremer, and B. Keimer, Phys. Rev. Lett. **105**, 027003 (2010).
- [23] L. Shan, Y.-L. Wang, J. Gong, B. Shen, Y. Huang, H. Yang, C. Ren, and H.-H. Wen, Phys. Rev. B **83**, 060510 (2011).
- [24] X. G. Luo, M. A. Tanatar, J.-P. Reid, H. Shakeripour, N. Doiron-Leyraud, N. Ni, S. L. Bud'ko, P. C. Canfield, H. Luo, Z. Wang, et al., Phys. Rev. B **80**, 140503 (2009).
- [25] J. Yang, D. Hüvonen, U. Nagel, T. Rõ om, N. Ni, P. C. Canfield, S. L. Bud'ko, J. P. Carbotte, and T. Timusk, Phys. Rev. Lett. **102**, 187003 (2009).
- [26] G. Li, W. Z. Hu, J. Dong, Z. Li, P. Zheng, G. F. Chen, J. L. Luo, and N. L. Wang, Phys. Rev. Lett. **101**, 107004 (2008).
- [27] A. Charnukha, O. V. Dolgov, A. A. Golubov, Y. Matiks, D. L. Sun, C. T. Lin, B. Keimer, and A. V. Boris (2011), arXiv:1103.0938v1.
- [28] H. Luo, Z. Wang, H. Yang, P. Cheng, X. Zhu, and H.-H. Wen, Superconductor Science and Technology **21**, 125014 (2008).
- [29] C. C. Homes, M. Reedyk, D. A. Cradles, and T. Timusk, Applied Optics **32**, 2976 (1993).
- [30] A. V. Puchkov, T. Timusk, W. D. Mosley, and R. N. Shelton, Phys. Rev. B **50**, 4144 (1994).
- [31] L. Degiorgi, E. J. Nicol, O. Klein, G. Grüner, P. Wachter, S.-M. Huang, J. Wiley, and R. B. Kaner, Phys. Rev. B **49**, 7012 (1994).
- [32] W. Zimmermann, E. Brandt, M. Bauer, E. Seider, and L. Genzel, Physica C: Superconductivity **183**, 99 (1991).
- [33] X. H. Zheng and D. G. Walmsley, Phys. Rev. B **77**, 104510 (2008).
- [34] H. Suhl, B. T. Matthias, and L. R. Walker, Phys. Rev. Lett. **3**, 552 (1959).
- [35] G. Mu, B. Zeng, P. Cheng, Z. S. Wang, L. Fang, B. Shen, L. Shan, C. Ren, and H. H. Wen, Chinese Phys. Lett. **27**, 037402 (2010).